HIF2α is an essential molecular brake for postprandial hepatic glucagon response independent of insulin signaling

Sadeesh K. Ramakrishnan[1], **Huabing Zhang**[1], **Shogo Takahashi**[4], **Brook Centofanti**[1], **Sarvesh Perisamy**[1], **Kevin Weisz**[1], **Zheng Chen**[1], **Michael D. Uhler**[2], **Liangyou Rui**[1], **Frank J. Gonzalez**[4], and **Yatrik M. Shah**[1,3]

[1]Department of Molecular & Integrative Physiology, University of Michigan Medical School, Ann Arbor, MI

[2]Department of Biological Chemistry, University of Michigan Medical School, Ann Arbor, MI

[3]Department of Internal Medicine, Division of Gastroenterology, University of Michigan Medical School, Ann Arbor, MI

[4]Center for Cancer Research, National Cancer Institute, National Institutes of Health, Bethesda, MD

Abstract

Glucagon drives hepatic gluconeogenesis and maintains blood glucose levels during fasting. The mechanism that attenuates glucagon action following refeeding is not understood. The present study demonstrates an increase in perivenous liver hypoxia immediately after feeding which stabilizes hypoxia-inducible factor (HIF)2α in liver. The transient postprandial increase in hepatic HIF2α attenuates glucagon signaling. Hepatocyte-specific disruption of HIF2α increases postprandial blood glucose and potentiates the glucagon response. Independent of insulin/AKT signaling, activation of hepatic HIF2α resulted in lower blood glucose, improved glucose tolerance and decreased gluconeogenesis due to blunted hepatic glucagon action. Mechanistically, HIF2α abrogated glucagon-PKA signaling by activating cAMP-phosphodiesterases in a MEK/ERK-dependent manner. Repression of glucagon signaling by HIF2α ameliorated hyperglycemia in streptozotocin-induced diabetes and acute insulin resistant animal models. This study reveals that HIF2α is essential for the acute postprandial regulation of hepatic glucagon signaling, and suggests HIF2α as a potential therapeutic target in the treatment of diabetes.
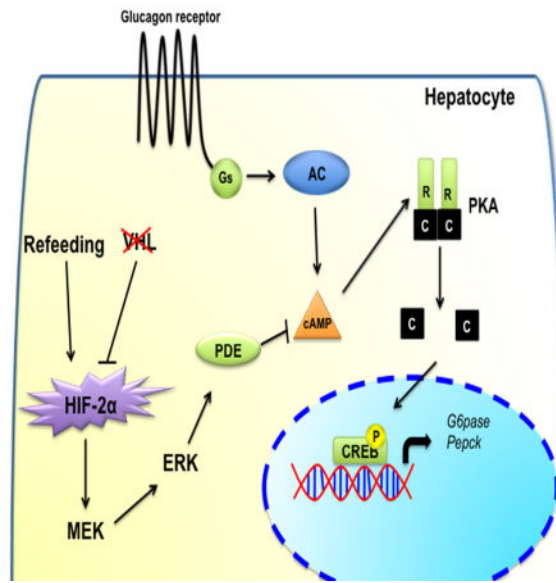
Graphical abstract

Correspondence: Yatrik M. Shah, Department of Molecular & Integrative Physiology, Department of Internal Medicine, Division of Gastroenterology, University of Michigan Medical, School, Ann Arbor, MI 48109. shahy@umich.edu.

Introduction

The counter regulatory hormone glucagon is involved in fasting energetics by promoting hepatic glucose output via gluconeogenesis and glycogenolysis (Habegger et al., 2010). Glucagon-mediated stimulation of protein kinase A (PKA)-cyclic AMP (cAMP) response element binding protein (CREB) signaling cascade, and dephosphorylation of CREB regulated transcriptional co-activator 2 (CRTC2) (Koo et al., 2005) increases the transcription of gluconeogenic genes, glucose 6 phosphatase (*G6pase*) and phosphoenolpyruvate carboxykinase (*Pepck*). During nutrient excess, glucagon action is attenuated by a decrease in glucagon secretion (Walker et al., 2011). However, there is a long delay in the return of glucagon back to basal levels following feeding (Unger et al., 1963). Sustained but controlled glucagon action during the post-absorptive phase is essential to prevent hypoglycemia after bolus of insulin release (Tse et al., 1983). Also, Glucagon priming is important for insulin effect on hepatic gluconeogenesis and glycogen synthesis (Lewis et al., 1997). However, dysregulated glucagon signaling results in hyperglycemia in type 2 diabetic patients with inappropriately high levels of glucagon (D'Alessio, 2011; Dunning and Gerich, 2007). Insulin partially attenuates glucagon signaling through phosphorylation and degradation of CRTC2 by SIK kinases (Dentin et al., 2007). However, the intracellular mechanisms involved in the regulation of glucagon-PKA-CREB signaling are largely unknown.

Chuvash polycythemia is a congenital oxygen sensing disorder that arises due to homozygous mutation of arginine to tryptophan in the von Hippel Lindau (VHL) protein resulting in decreased ability of VHL to bind and degrade hypoxia-inducible factor (HIF)

(Ang et al., 2002; Hickey et al., 2007). HIF1α and HIF2α are the two major HIF isoforms that regulate numerous genes involved in cell survival, glucose metabolism, inflammation, angiogenesis and erythropoiesis (Ackerman and Simon, 2014; Prabhakar and Semenza, 2015; Zheng et al., 2015). One of the common clinical manifestations in Chuvash polycythemia is hypoglycemia (McClain et al., 2013). Recent studies demonstrated that activation of hepatic HIF2α in the liver increases insulin sensitivity and improves glucose homeostasis via activation of the insulin receptor substrate (IRS2)-AKT signaling pathway (Taniguchi et al., 2013; Wei et al., 2013). However, hypoglycemia in Chuvash polycythemic patients, even in the presence of high levels of gluconeogenic substrates such as glycerol, lactate and pyruvate, suggests the possibility of altered glucagon action (Formenti et al., 2010; Jenssen et al., 1990).

In this study, we demonstrate that feeding leads to a rapid and transient hypoxia in the liver, which through HIF2α is essential in regulating the hepatic glucagon response. Disruption of HIF2α increases postprandial glucose levels and hepatic glucagon action. Conversely, activation of hepatic HIF2α abrogated glucagon action and decreases gluconeogenesis through increased phosphodiesterase (PDE)4 activity. This study demonstrates that HIF2α is a potential therapeutic target in the treatment of diabetes.

Results

Disruption of hepatic VHL improves glucose homeostasis with a parallel decrease in glucagon action

To understand the role of HIF signaling in glucose homeostasis, mice with disruption of VHL in liver (Vhl^{LivKO}) using a tamoxifen-inducible Cre recombinase under the control of the albumin promoter were assessed (Qu et al., 2011). Vhl^{LivKO} mice had lower fasting glucose levels with a progressive improvement in glucose tolerance at 1- and 2-weeks following Vhl disruption (Figure 1A and B, and Figure S1A). HIF2α in the liver improves glucose homeostasis via IRS2-insulin signaling (Taniguchi et al., 2013; Wei et al., 2013); however, IRS2 mRNA and/or protein levels were not increased at 1-week but increased at 2-weeks or later following Vhl disruption (Figure S1B–D). In addition, insulin stimulated AKT phosphorylation was not different between primary hepatocytes (PH) from Vhl^{LivKO} and $Vhl^{F/F}$ mice (Figure 1C). Expression of $G6pase$ and $Pepck$ were significantly decreased in PH from Vhl^{LivKO} mice, which could not be restored by the PI3K inhibitor, Wortmannin (Figure 1D). FOXO1, a critical regulator of gluconeogenesis, which is excluded from the nucleus through AKT-mediated phosphorylation, was increased in nuclear lysates of hepatocytes from Vhl^{LivKO}, possibly a compensatory mechanism to circumvent hypoglycemia (Figure S1E). Moreover, no difference in insulin tolerance at 1-week (Figure 1E), suggests that additional mechanisms exists in parallel to the IRS2/AKT pathway that accounts for the improved glucose homeostasis in Vhl^{LivKO} mice. Induction of hepatic $G6pase$ upon fasting was completely abrogated in the livers of Vhl^{LivKO} mice, while $Pepck$ mRNA was significantly attenuated (Figure 1F and G). Further analysis revealed a progressive decrease in glucagon response starting at 1-week, and complete abrogation at 2-weeks following VHL disruption (Figure 1H and Figure S1F). A significant decrease in insulin levels (Figure 1I), and elevation in plasma glucagon levels (Figure 1J) resulted in a

lower insulin:glucagon ratio (0.008 in Vhl^{LivKO} mice compared to 0.003 in $Vhl^{\text{F/F}}$ mice). Together this data indicates that the decrease in hepatic glucagon action may be responsible for improved glucose homeostasis in Vhl^{LivKO} mice.

Disruption of hepatic VHL decreases glucagon mediated glucose output in the liver

Hepatic gluconeogenesis, assessed by a pyruvate tolerance test, revealed a progressive decrease in glucose output in Vhl^{LivKO} mice at 1- and 2-weeks following VHL disruption (Figure 2A and Figure S2A). A significant decrease in the hepatic G6Pase enzyme activity with a concomitant increase in glycogen content was observed in the Vhl^{LivKO} mice (Figure 2B and C). In addition, both basal and glucagon-induced glucose production were significantly decreased in PH from Vhl^{LivKO} mice (Figure 2D). Moreover, induction of *G6pase* and *Pepck* mRNA and protein by glucagon were completely abrogated in Vhl^{LivKO} PH (Figure 2E and F). As a positive control, expression of the HIF2α target gene erythropoietin (*Epo*) was highly induced in the Vhl^{LivKO} PH (Figure 2E). To determine if IRS2/AKT has any role in the glucagon resistance of Vhl^{LivKO} mice, PH were pretreated with PI3K inhibitor (Wortmannin and LY294002) and an allosteric AKT inhibitor (MK-2206). Inhibiting IRS2/AKT did not restore glucagon induction of *G6pase* mRNA levels and hepatic glucose production in Vhl^{LivKO} PH suggesting that glucagon resistance is independent of AKT signaling in Vhl^{LivKO} mice (Figure 2G–I and S2B). Further, adenoviral *G6pase* promoter luciferase assay revealed a complete loss of glucagon induction of *G6pase* promoter activity in Vhl^{LivKO} PH (Figure 2J). PGC-1α is an important transcription co-factor required for *G6pase* and *Pepck* expression (Herzig et al., 2001). However, a decreased PGC-1α expression in Vhl^{LivKO} mice is not responsible for the lower blood glucose, as adenoviral-mediated PGC-1α expression did not restore glucagon effect on *G6pase* expression (Figure S2C and S2D). Dexamethasone induction of gluconeogenic genes was not altered in Vhl^{LivKO} PH (Figure 2K), suggesting a specific abrogation of glucagon signaling. Disruption of VHL in PH led to induction of STAT3 signaling (Figure S2E), which can inhibit gluconeogenesis (Ramadoss et al., 2009). However STAT3 inhibitors, which completely blocked phospho-STAT3, could not restore induction of *G6pase and Pepck* mRNA expression by glucagon in Vhl^{LivKO} PH (Figure S2F and S2G). To further dissect the mechanism of blunted glucagon action in Vhl^{LivKO} mice, glucagon stimulated CREB phosphorylation was assessed. Treatment with glucagon induced CREB phosphorylation in $Vhl^{\text{F/F}}$ but not Vhl^{LivKO} mice, both in vivo and in PH (Figure 2L and M). Taken together, these data suggest that Vhl^{LivKO} mice exhibit decreased glucose output due to blunted glucagon-CREB signaling in the liver.

Activation of HIF2α decreases hepatic glucagon action

To determine whether the decrease in hepatic glucagon action was mediated by HIF1α or HIF2α, mice with compound disruption of VHL and HIF1α ($Vhl/Hif1α^{\text{LivKO}}$) or VHL and HIF2α ($Vhl/Hif2α^{\text{LivKO}}$) were examined. Lower blood glucose levels in Vhl^{LivKO} mice were completely reversed by the loss of both VHL and HIF2α, but not VHL and HIF1α (Figure 3A and Figure S3A). The plasma insulin levels were increased and serum glucagon levels were normalized in $Vhl/Hif2α^{\text{LivKO}}$ mice (Figure 3B). Fasting *G6pase* and *Pepck* mRNA levels were restored in $Vhl/Hif2α^{\text{LivKO}}$ mice (Figure 3C). Further, the improvement in glucose homeostasis following VHL disruption was completely reversed in $Vhl/Hif2α^{\text{LivKO}}$

but not in *Vhl/Hif1α*^{LivKO} mice (Figure 3D and Figure S3B). Insulin tolerance test revealed no difference in the insulin sensitivity between *Vhl*^{F/F}, *Vhl*^{LivKO}, and *Vhl/Hif2α*^{LivKO} mice (Figure 3E). Additionally, glucagon response and gluconeogenesis in *Vhl/Hif2α*^{LivKO} mice were comparable to *Vhl*^{F/F} mice, but not in *Vhl/Hif1α*^{LivKO} mice (Figure 3F and G and Figure S3C and S3D). Interestingly, blood glucose levels were higher during the glucagon and pyruvate tolerance test in *Vhl/Hif2*^{LivKO} mice (Figure 3F and G). Combined loss of HIF2α and VHL completely restored the glucagon-mediated induction of *G6pase* and *Pepck* mRNAs (Figure 3H) and CREB phosphorylation (Figure 3I), to levels similar as in PH from *Vhl*^{F/F} mice. Taken together, these data suggest that the improvement in glucose homeostasis and attenuated glucagon action in *Vhl*^{LivKO} mice is HIF2α dependent.

Activation of HIF2α is critical to regulate postprandial glucose levels

To determine the role of dietary status on hepatic HIF signaling, hypoxia reporter mice (ODD-Luc; (Shah et al., 2008)) were fasted for 16-hours and then refed for 30, 60 and 120 minutes. Refeeding increased plasma insulin levels with a corresponding increase in AKT phosphorylation (Figure S4A and S4B). Refeeding significantly decreased the levels of pCREB as well as *G6pase* and *Pepck* mRNA (Figure S4B and S4C). When assessed by the IVIS in vivo luciferase imaging system, refeeding after overnight fasting resulted in a robust increase in HIF expression, which was visualized at 30 minutes after refeeding, and persisted until 120 minutes (Figure 4A). Similarly, tissue luciferase in the livers of ODD-luc mice demonstrated increased luciferase activity at 30, 60 and 120 minutes after refeeding (Figure 4B). Further, Western blot analysis revealed induction of HIF2α expression in the nucleus of livers from refed mice (Figure 4C). Fasting increases hepatic blood circulation possibly to mobilize glucose (Eipel et al., 2010; Exton et al., 1972). Upon refeeding, the central blood circulation is directed towards intestine to facilitate nutrient absorption (Gallavan and Chou, 1985). However, it is not known whether the re-routing of circulation by refeeding affects hepatic oxygen dynamics. To determine hypoxic activation of HIF2α after refeeding from a hypoxic-independent increase of HIF2α, mice were injected with the hypoxyprobe (a pimonidazole compound which forms adducts in hypoxic cells) and then refed for 30 or 60 minutes. Immunostaining revealed a significant elevation in pimonidazole adducts at 30 and 60 minutes after refeeding in the hepatocytes surrounding the central vein, with a concomitant co-localization of HIF2α (Figure 4D), suggesting that refeeding-induced transient hypoxia stabilizes HIF2α in hepatocytes. The physiological role of HIF2α in hepatic glucagon signaling was further elucidated using mice with a temporal disruption of HIF2α in the liver (*Hif2α*^{LivKO}) by tamoxifen-inducible Cre recombinase expressed from the albumin promoter. Tamoxifen treatment significantly decreased HIF2α expression in the hepatocytes (Figure 4E). Glucose tolerance test was not different in *Hif2α*^{LivKO} mice (Figure 4F); however, the glucagon response was significantly increased in *Hif2α*^{LivKO} similar to *Vhl/Hif2α*^{LivKO} mice (Figure 4G). To determine the role of HIF2α in postprandial glucose homeostasis, a fasting-refeeding experiment was performed. A modest but significant increase in the postprandial glucose levels were observed in *Hif2α*^{LivKO} mice (Figure 4H). Refeeding induced AKT phosphorylation to similar level; however, phosphorylated CREB was significantly elevated at all time points of refeeding in *Hif2α*^{LivKO} livers (Figure 4I). Collectively, these data suggests that the transient increase in

hepatic HIF2α after refeeding has a critical role in the regulation of postprandial glucose homeostasis by repressing glucagon-CREB signaling in liver.

Glucagon stimulated PKA activation is attenuated in Vhl^{LivKO} mice

To determine the mechanism by which HIF2α represses glucagon signaling, PH were pretreated with the phosphatase inhibitor okadaic acid (OKA). Okadaic acid did not restore glucagon stimulated CREB phosphorylation or *G6pase* promoter activity in the PH from *Vhl*^{LivKO} mice (Figure 5A and Figure S5A). Interestingly, reconstituting *Vhl*^{LivKO} PH lysate with recombinant PKA induced CREB phosphorylation, suggesting that PKA activity may be repressed in *Vhl*^{LivKO} mice (Figure S5B). Further analysis revealed a significant decrease in glucagon-induced PKA activity in *Vhl*^{LivKO} PH (Figure 5B). These data are consistent with decreased glucagon-induced pan-phoshoPKA substrates (Figure 5C). PKA is a holoenzyme made up of four subunits; two regulatory and two catalytic subunits (Kim et al., 2007). qPCR analysis revealed that the regulatory subunit II-beta (PKA-RIIβ) mRNA is significantly increased, whereas the catalytic subunit alpha (PKA-Cα) mRNA is decreased in the *Vhl*^{LivKO} livers (Figure S5C). Western blot analysis revealed no difference in the protein levels of PKA-RI or the PKA-Cα subunits; however, there was a significant decrease in PKA-RII subunit (Figure S5D). Disruption of VHL did not affect nuclear PKA-Cα levels or binding of PKA-Cα to CREB (Figure S5E–G). Although regulators of PKA such as A-kinase anchoring protein (AKAP)-12 and Syk were significantly increased in *Vhl*^{LivKO} livers, AKAP12 modulator (phorbol myristate acetate, PMA) or Syk inhibitor (piceatannol) did not restore glucagon induction of *Pepck* and *G6pase* mRNA levels (Figure S5H–J), suggesting that the decrease in PKA activity is not due to disproportionate levels of PKA subunits. Increase in intracellular cAMP is a key event in the activation of PKA-CREB signaling cascade. Glucagon treatment resulted in a ~10-fold increase in intracellular cAMP levels in *Vhl*$^{F/F}$ PH, which was significantly attenuated in *Vhl*^{LivKO} mice (Figure 5D). Forskolin, a direct and potent activator of adenyl cyclase, increased CREB phosphorylation and *G6pase* and *Pepck* expression in *Vhl*$^{F/F}$ PH but not in *Vhl*^{LivKO} PH (Figure 5E and Figure S5K). However, treatment with a stable 8-br-cAMP completely restored PKA-CREB signaling (Figure 5F and Figure S5L–M). Collectively, these data suggest that HIF2α inhibits glucagon-PKA signaling by affecting the intracellular cAMP levels.

Inhibiting PDE activity restores glucagon sensitivity in hepatocytes from Vhl^{LivKO} mice

Intracellular cAMP levels are tightly regulated by PDEs. To further investigate the mechanism, PDE activity was assessed in PH, which revealed that PDE activity is significantly elevated in *Vhl*^{LivKO} PH (Figure 5G). Pan-PDE inhibitor IBMX (3-isobutyl-1-methyl xanthine) restored glucagon-stimulated CREB phosphorylation, PKA substrate phosphorylation, and expression of *G6pase* and *Pepck* mRNAs in *Vhl*^{LivKO} PH (Figure 5H and I and Figure S5N). In addition, glucagon induced cAMP levels were comparable between *Vhl*$^{F/F}$ and IBMX-treated *Vhl*^{LivKO} PH (Figure 5J). Mammalian PDEs are composed of 21 genes and grouped into 11 isoforms based on their sequence homology, property and regulation (Omori and Kotera, 2007). PDE4 plays an important role in hepatic glucagon signaling (Abdollahi et al., 2003). To assess whether PDE4 is involved in HIF2α regulation of glucagon signaling, PH were pre-treated with PDE4 specific inhibitors Rolipram, Glaucine, Ibudilast, or CP80,633 and then treated with glucagon. Inhibiting PDE4

restored glucagon stimulated CREB phosphorylation and expression G6Pase and PEPCK in Vhl^{LivKO} PH (Figure 5K–L). However, PDE2, 3 or 10 inhibitors did not restore glucagon signaling (Figure S5O). Interestingly, gene expression analysis revealed a significant increase in $Pde1b$, $Pde2a$, $Pde3a$ and $Pde7b$ mRNAs in Vhl^{LivKO} PH in a HIF2α-dependent manner, but not mRNA or protein levels of PDE4 (Figure S5P–R), suggesting that HIF2α potentially regulates PDE4 activity through post-translation modification.

HIF2α activated ERK signaling represses hepatic glucagon action

To delineate the pathway upstream of PDE4 in HIF2α regulation of glucagon signaling, we screened for glucagon induced $G6pase$ expression in the $Vhl^{F/F}$ and Vhl^{LivKO} PH in the presence of various inhibitors or activators of key signaling pathways, which were shown to regulate PDE activity or glucagon signaling (Omori and Kotera, 2007). Interestingly, among the various compounds tested, SRC inhibitor (SU6656), MEK inhibitors (GSK1120212 and PD98059) and ERK inhibitor (FR180204) partially restored glucagon induced $G6pase$ expression in the Vhl^{LivKO} PH (Figure 6A). Further analysis revealed a significant increase in the phosphorylation of p42/p44 ERK in the livers and PH of Vhl^{LivKO} mice (Figure 6B). Inhibiting p42/p44 ERK using MEK inhibitors (GSK and PD) and ERK inhibitor (FR) partially restored glucagon induced CREB phosphorylation and PKA inhibitor H-89 inhibited the glucagon effect in Vhl^{LivKO} PH (Figure 6C and D). Similarly, MEK or ERK inhibitors increased glucagon induced $G6pase$ expression by ~10 fold in Vhl^{LivKO} PH, which is comparable to the induction observed in $Vhl^{F/F}$ PH (Figure 6E). Inhibiting MEK/ERK also restored glucagon-induced glucose output in Vhl^{LivKO} PH (Figure 6F). Similarly, adenoviral-mediated overexpression of dominant negative MEK1 (Ad-MEK1DN) partially restored glucagon-stimulated $G6pase$ expression in Vhl^{LivKO} PH (Figure S6A), suggesting that ERK is a critical regulator of hepatic glucagon signaling in Vhl^{LivKO} mice. Adenovirus-mediated expression of constitutive active MEK-ERK (Ren et al., 2010) decreased glucagon-stimulated CREB phosphorylation and induction of $G6pase$ and $Pepck$ mRNAs in WT PH (Figure 6G and H). Activation of MEK-ERK resulted in increased PDE activity (Figure 6I). Through screening we observed that inhibiting SRC kinase could partially restore glucagon induced $G6pase$ expression in PH from Vhl^{LivKO} mice (Figure 6A); however, hepatic glucose production in Vhl^{LivKO} PH was not further improved by SRC kinase inhibitor (Figure S6B). HIF2α-mediated ERK phosphorylation has been shown to be potentiated by EGFR signaling (Wang and Schneider, 2010). To determine whether ERK activation requires HIF2α transcription activity, mice with compound disruption of VHL and aryl hydrocarbon nuclear translocator (ARNT; $Vhl/Arnt^{LivKO}$ mice) were examined. HIF heterodimerization with ARNT is essential to activate its target gene expression. No difference in ERK phosphorylation, blood glucose levels or $G6pase$ and $Pepck$ mRNA levels in $Vhl/Arnt^{LivKO}$ mice (Figure S6C–E), suggests that HIF2α transcriptional activity is essential for ERK regulation of gluconeogenesis. Collectively, these data demonstrate that the HIF2α attenuates glucagon response partially by activating ERK signaling.

HIF2α mediated glucagon resistance ameliorates hyperglycemia in diabetic mouse models

The present study together with previous work clearly demonstrates that activation of hepatic HIF2α increases insulin sensitivity (Taniguchi et al., 2013) and dampens glucagon response. However, to date, an essential role for hepatic HIF2α in diet-induced glucose

intolerance has not been studied. Therefore, metabolic parameters were assessed in $Hif2\alpha^{\text{LivKO}}$ and littermate controls that were fed a high-fat diet for 6-weeks. No significant difference was observed in glucose and insulin tolerance test between $Hif2\alpha^{\text{LivKO}}$ and littermate controls (Figure 7A and B). However, $Hif2\alpha^{\text{LivKO}}$ mice exhibited an increased glucagon response (Figure 7C). Although HIF2α regulation of glucagon signaling was not an essential protective mechanism, HIF2α is sufficient in improving diabetic parameters in diet- and genetic-induced obesity models through activation of the IRS2/AKT pathway (Taniguchi et al., 2013; Wei et al., 2013). To rule-out the confounding effect of insulin and to determine if ablation of glucagon response by VHL disruption would ameliorate hyperglycemia, we assessed glucose levels in streptozotocin (STZ)-induced diabetic mouse model and an acute insulin resistant model. Diabetes was first induced by STZ administration and then hepatic VHL was disrupted using tamoxifen (Figure 7D). STZ treatment decreased the serum insulin levels, islet size, and islet insulin content with no obvious changes in islet glucagon content (Figure S7A and S7B). Consistent with glucagon resistance, a significant increase in serum glucagon levels was observed, resulting in a lower insulin:glucagon ratio in Vhl^{LivKO} mice when compared to $Vhl^{\text{F/F}}$ and $Vhl/Hif2^{\text{LivKO}}$ (Figure S7C and S7D). A significant increase in the blood glucose was observed at 5-days after STZ treatment (Figure 7D), and following 6-days after tamoxifen injection, blood glucose levels returned to normal in the Vhl^{LivKO} mice, whereas the blood glucose remained highly elevated in $Vhl/Hif2^{\text{LivKO}}$ and $Vhl^{\text{F/F}}$ mice (Figure 7D). Further analysis revealed a significant decrease in the expression of *G6pase* and *Pepck* mRNA in the livers of Vhl^{LivKO} mice (Figure 7E). In addition, inducing acute insulin resistance using MK-2206, the first allosteric AKT inhibitor approved for the treatment of solid tumors in humans (Yap et al., 2011), transiently increased blood glucose levels (Cherrin et al., 2010; Yap et al., 2011) in $Vhl^{\text{F/F}}$ and $Vhl/Hif2^{\text{LivKO}}$ mice, but not in Vhl^{LivKO} (Figure 7F). Taken together, these data revealed that disruption of VHL improves glucose homeostasis in both insulin deficient and insulin resistant animal models by attenuating hepatic glucagon response.

Discussion

Glucagon has a central role in maintaining fasting blood glucose levels, as well as in metabolic diseases such as type II diabetes (D'Alessio, 2011; Dunning and Gerich, 2007). Decreasing glucagon signaling improves glucose homeostasis (Conarello et al., 2007; Lee et al., 2011; Liang et al., 2004). However, very little is known about the mechanisms that regulate hepatic glucagon signaling. The present work demonstrates that a transient postprandial increase in hepatic HIF2α acts as a critical molecular brake for glucagon signaling. During fasting, circulation to liver is increased to channel lactate for gluconeogenesis (Eipel et al., 2010; Exton et al., 1972). Upon refeeding, the diversion of blood supply towards intestine (Gallavan and Chou, 1985) induces a transient perivenous hypoxia sufficient to stabilize HIF2α in liver. Mechanistically, HIF2α repressed postprandial glucagon response and gluconeogenesis by increasing PDE activity and cAMP hydrolysis in an ERK dependent manner (Figure 7G). Suppression of glucagon action after refeeding is important under conditions such as type-1-diabetes and insulin resistance (Baron et al., 1987; Porksen et al., 2007). Repression of hepatic glucagon signaling by HIF2α is sufficient to ameliorate hyperglycemia in STZ-induced type-1 diabetes and AKT

inhibitor driven acute insulin resistant mouse models. Currently, insulin signaling is the best-known counter-regulatory mechanism to glucagon signaling. The present work demonstrates that HIF2α inhibits glucagon signaling by a parallel pathway, independent of insulin signaling. However, systemic glucose levels continue to decrease at 2-weeks following HIF2α activation, which might be contributed in part by an increase in insulin sensitivity, as IRS2 levels were elevated at 2-weeks following VHL disruption. Thus, HIF2α regulation of hepatic insulin and glucagon pathways may work synergistically. Current work is aimed in understanding the integration of glucagon and insulin signaling by HIF2α.

Vhl^{LivKO} mice exhibit increased levels of EPO, lower hepcidin levels, increased erythropoiesis and polycythemia (Anderson et al., 2012), similar to $Vhl^{R/R}$ mice that carry a homozygous mutation (R200W) observed in Chuvash polycythemia (Gordeuk et al., 2011; Hickey et al., 2007). This work suggests a potential mechanism by which Chuvash polycythemia patients have lower blood glucose through HIF2α regulation of glucagon signaling, as no change in insulin sensitivity was observed in these patients. Although it is possible that the hypoglycemia in Chuvash polycythemia patients may be caused by impaired glucagon signaling, it should be noted that the increase in HIF2α is robust in the mouse model with VHL disruption compared to the modest HIF2α increase in Chuvash polycythemia patients and $Vhl^{R/R}$ mice. Therefore, at this time we cannot completely rule out the confounding glucose lowering effects by polycythemia in our mouse model.

cAMP levels determine the activation of the PKA signaling. Restoration of glucagon signaling by PDE4 inhibitors demonstrates a central role for PDE4 in the regulation of hepatic glucagon signaling by hypoxia. However, PKA-RII subunit is significantly decreased in the livers of the Vhl^{LivKO} mice. Genetic ablation of the PKA regulatory subunit results in loss of cAMP stimulated PKA response, and constitutive activation of PKA signaling (Cummings et al., 1996). However, there is no increase in basal PKA signaling, and 8-br-cAMP treatment induces CREB signaling and gluconeogenic gene expression in Vhl^{LivKO} mice. Therefore, we believe that the decrease in PKA-RII subunit may be a compensatory mechanism to promote PKA signaling, rather to repress glucagon signaling. PDE4 is the largest of the mammalian PDE family members, comprised of 4 genes and over 18 variants (Omori and Kotera, 2007). Among them, PDE4D has been well characterized to be a critical regulator of hepatic glucagon signaling. PDE4D activity is regulated by ERK through phosphorylation (MacKenzie et al., 2000). ERK phosphorylation is highly induced in the liver and PH from Vhl^{LivKO} mice, which is sufficient to abolish glucagon signaling through increases in PDE activity. It should be noted that inhibiting PDE4 or ERK activity did not fully restore glucagon signaling to the levels observed with the pan-PDE inhibitor IBMX, suggesting that other PDEs and/or signaling pathways might be involved in the HIF regulation of glucagon signaling. Moreover, overexpression of constitutive active MEK-ERK only resulted in modest increase in the total PDE activity as compared to activation of HIF2α. This may suggests that ERK selectively increases PDE4 activity, which in turn ablates glucagon signaling, whereas HIF2α could increase global PDE activity by mechanisms that are currently unknown. Indeed, PDE1B, 2A, 3A, 7B and 10A were increased in liver in a HIF2α dependent manner.

The importance of glucagon in the pathogenesis of diabetes is well characterized. Increased glucagon signaling leads to dysregulated glucose homeostasis, whereas a decrease in glucagon action improves glycemic index in diabetes independent of insulin sensitivity (Baron et al., 1987; Conarello et al., 2007; D'Alessio, 2011; Dunning and Gerich, 2007; Gelling et al., 2003; Lee et al., 2011; Liang et al., 2004). In this study, HIF2α was found to have a beneficial effect on glucose homeostasis in part by repressing hepatic glucagon signaling and other studies have demonstrated that HIF2α increases insulin signaling (Taniguchi et al., 2013; Wei et al., 2013). FG-4592, a PHD inhibitor that stabilizes HIF2α is under phase III clinical trial for the treatment of anemia in chronic kidney disease patients. FG-4592 or other PHD inhibitors could be highly beneficial in improving glucose homeostasis in diabetic patients through HIF2α-dependent mechanisms.

Experimental Procedures

Animals and Diets

$Vhl^{F/F}$, Vhl^{LivKO} $Vhl/Hif1\alpha^{F/F}$, $Vhl/Hif1\alpha^{LivKO}$, $Vhl/Hif2\alpha^{F/F}$, $Vhl/Hif2\alpha^{LivKO}$, $Vhl/Arnt^{F/F}$ and $Vhl/Arnt^{LivKO}$ were described previously (Anderson et al., 2012; Qu et al., 2011). For temporal hepatocyte-specific disruption of HIF2α, $HIF2\alpha^{F/F}$ mice on a C57BL/6 background were crossed with mice harboring the cre-ER^{T2} recombinase under albumin promoter, SA-Cre-ER^{T2} (Schuler et al., 2004). Wild-type littermates ($HIF2\alpha^{F/F}$) were used as control. $HIF2\alpha^{F/F}$ and $HIF2\alpha^{LivKO}$ were fed with either normal chow or 60% high fat diet (Research diets, New Brunswick, NJ). For hypoxyprobe experiment, animals were fasted overnight and then injected intraperitoneally (i.p.) with 60 mg/kg pimonidazole, followed by refeeding for 30 minutes. For inducing hyperglycemia, mice were starved for four hours and then injected with STZ i.p. at a dose of 50 mg/kg body weight for five consecutive days or treated with 50 mg/kg MK-2206. All mice were housed at the Unit for Laboratory Animal Management (ULAM) at the University of Michigan. All animal procedures were approved by the University of Michigan Institutional Animal Care and Utilization Committee (IACUC). All mice were fed *ad-libitum* and kept in a 12-hour dark/light cycle with chow replenished every week.

Metabolic tests

For glucose and pyruvate tolerance test, mice on regular chow diet or high-fat diet were fasted for 16-hours and for insulin and glucagon tolerance test, mice were fasted for 6- and 5- hours, respectively. Fasted blood glucose was measured from the tail vein by tail snipping and then glucose (1.5 g/kg body weight), human insulin (Humulin, Eli and Lilly, Indianapolis, IN) (0.75 U/kg body weight), glucagon (15 μg/kg body weight) or pyruvate (2 g/kg body weight) was administered i.p. to conscious animals. Glucose was measured in blood taken from the tail vein at 15, 30, 45, 60 and 120 min post-injection.

Insulin and glucagon assay

Insulin assay and glucagon assay were performed using EIA kit from Crystal Chem (Downers Grove, IL) and RIA kit from Millipore (Temecula, CA), respectively, using manufacturers protocol.

PH isolation and treatment

PH were isolated from mice on normal chow diet at 1-week after tamoxifen treatment, unless otherwise mentioned. Briefly, livers were perfused with 10 ml of EBSS containing 0.5 mM EGTA, followed by perfusion with William's E media containing collagenase type II (Worthington, Lakewood, NJ). Viable cells were plated in Williams E media with 10% FBS. For glucagon treatment, PH were serum starved overnight and treated with 50 nM glucagon for 2-hours (for RNA analysis) or 10-minutes (for protein studies). For inhibitor or activator studies, PH were pre-treated for 4-hours with FT13a (apelin inhibitor), Oligomycin (mitochondrial ATP synthase inhibitor), Wortmannin (PI3Kinase inhibitor), Ad-HT31 (AKAP inhibitor), WY14643 (PPARα agonist), Ad-HNF4, KN62 (CamKinase II inhibitor), FIPI (Phospholipase D inhibitor), PLA2 (Phospholipase A inhibitor), Anti-vascular growth factor a (Vegfa Ab), DEA (Diethylamine), DETA (Diethylenetriamine), GMP (8-br-cGMP), Rotenone (ETC inhibitor), Thapsigargin (ER stress inhibitor), tBHQ (tert-butylhydroquinone), 2-deoxyglucose, SU6656 (SRC kinase inhibitor), MEK inhibitor (GSK1120212 and PD98059) and FR180204 (ERK inhibitor). For PDE4 inhibitors, PH were treated with Rolipram, Glaucine, Ibudilast, and CP80,633 for 16-hours and then again treated with additional 1 μM of respective PDE inhibitors for 30 minutes before glucagon treatment. For adenoviral infection, 5-hours after plating, PH were infected with 100 MOI adenoviral particles for 48-hours or as noted in the figure legends. Ad-G6Pase luciferase virus was kind gift from Dr. Marc Montminy, Ad-MEK-ERK-LA was a kind gift from Dr. Michael Simons (Yale University, New Haven, CT), and dominant negative MEK1 adenovirus was purchased from Cell Biolabs (San Diego, CA). For luciferase assay, 16-hours post infection, PH were treated with 50 nM glucagon or 8-bromo cAMP (250 μM or 500 μM) in Williams E media without FBS for 24-hours. The cells were washed twice with PBS and lysed in reporter lysis buffer (Promega, Madison, WI) and luciferase activity were normalized to protein content.

Hepatic glucose production

Hepatocytes cultured overnight were washed with PBS and then incubated with KRB buffer for 2 hours. Following incubation, 0.5 mM pyruvate and 1mM lactate were added to the KRB buffer with or without 50 nM glucagon and incubated at 37C for additional 4-hours. Glucose release was measured using glucose kit (Stanbio Laboratories, Boerne, TX).

Cyclic AMP assay

PH were serum starved overnight, treated with 50 nM glucagon for 10 minutes and then lysed with 0.1M HCl. cAMP was measured using EIA kit (Cayman chemicals, Ann Arbor, MI).

PKA activity assay

Following overnight serum starvation, PH were treated with 50nM glucagon and lysed in MOPS buffer with protease and phosphatase inhibitor. PKA activity assay was performed following manufacturers protocol (Enzo lifesciences, Farmingdale, NY).

PDE activity assay

PDE activity was assessed in PH using PDE activity assay kit following manufacturers protocol (Abcam, Cambridge, MA).

Real-time PCR

Total RNA was reverse transcribed, and the relative amount of individual mRNA was calculated after normalizing to their corresponding β-actin mRNA, as previously described (Ramakrishnan et al., 2015). Primer sequences are included in Table S1.

Western blot

Whole cell or nuclear lysates prepared as described before (Ramakrishnan et al., 2015) were separated by SDS-PAGE, transferred to nitrocellulose membrane and probed overnight at 4C with antibodies for pCREB, CREB, pERK, ERK, pAKT, AKT, pSTAT3, pPKA substrate, STAT3, PKA-R1α/β, PKA-Cα (Cell Signaling, Danvers, MA), Lamin B1, PDE4D (Abcam,), Lamin A/C (Active motif), G6pase, Pepck, AKAP-12, GAPDH (Santa Cruz, Dallas, TX) and HIF2α (Novus, Littleton, CO) and, PKA-RII (a kind gift from Dr. Michael Uhler, University of Michigan). Densitometry of the immunoblots were done using image-J software and expressed as fold change from the control or vehicle treated samples.

Immunostaining

Frozen sections were probed with polyclonal rabbit anti-HIF2α antibody (Novus) or Hypoxyprobe (Burlington, MA) as previously described (Ramakrishnan et al., 2015).

Statistical analysis

Results are expressed as mean ± SEM. Significance among multiple groups were tested using one-way analysis of variance followed by Dunnett's *post-hoc* for multiple comparisons and significance between two groups were calculated by Independent t-test.

Supplementary Material

Refer to Web version on PubMed Central for supplementary material.

Acknowledgments

References

Abdollahi M, Chan TS, Subrahmanyam V, O'Brien PJ. Effects of phosphodiesterase 3,4,5 inhibitors on hepatocyte cAMP levels, glycogenolysis, gluconeogenesis and susceptibility to a mitochondrial toxin. Molecular and cellular biochemistry. 2003; 252:205–211. [PubMed: 14577594]

Ackerman D, Simon MC. Hypoxia, lipids, and cancer: surviving the harsh tumor microenvironment. Trends Cell Biol. 2014; 24:472–478. [PubMed: 24985940]

Anderson ER, Taylor M, Xue X, Martin A, Moons DS, Omary MB, Shah YM. The hypoxia-inducible factor-C/EBPalpha axis controls ethanol-mediated hepcidin repression. Mol Cell Biol. 2012; 32:4068–4077. [PubMed: 22869521]

Ang SO, Chen H, Hirota K, Gordeuk VR, Jelinek J, Guan Y, Liu E, Sergueeva AI, Miasnikova GY, Mole D, Maxwell PH, Stockton DW, Semenza GL, Prchal JT. Disruption of oxygen homeostasis underlies congenital Chuvash polycythemia. Nature genetics. 2002; 32:614–621. [PubMed: 12415268]

Baron AD, Schaeffer L, Shragg P, Kolterman OG. Role of hyperglucagonemia in maintenance of increased rates of hepatic glucose output in type II diabetics. Diabetes. 1987; 36:274–283. [PubMed: 2879757]

Cherrin C, Haskell K, Howell B, Jones R, Leander K, Robinson R, Watkins A, Bilodeau M, Hoffman J, Sanderson P, Hartman G, Mahan E, Prueksaritanont T, Jiang G, She QB, Rosen N, Sepp-Lorenzino L, Defeo-Jones D, Huber HE. An allosteric Akt inhibitor effectively blocks Akt signaling and tumor growth with only transient effects on glucose and insulin levels in vivo. Cancer biology & therapy. 2010; 9:493–503. [PubMed: 20139722]

Conarello SL, Jiang G, Mu J, Li Z, Woods J, Zycband E, Ronan J, Liu F, Roy RS, Zhu L, Charron MJ, Zhang BB. Glucagon receptor knockout mice are resistant to diet-induced obesity and streptozotocin-mediated beta cell loss and hyperglycaemia. Diabetologia. 2007; 50:142–150. [PubMed: 17131145]

Cummings DE, Brandon EP, Planas JV, Motamed K, Idzerda RL, McKnight GS. Genetically lean mice result from targeted disruption of the RII beta subunit of protein kinase A. Nature. 1996; 382:622–626. [PubMed: 8757131]

D'Alessio D. The role of dysregulated glucagon secretion in type 2 diabetes. Diabetes, obesity & metabolism. 2011; 13(Suppl 1):126–132.

Dentin R, Liu Y, Koo SH, Hedrick S, Vargas T, Heredia J, Yates J 3rd, Montminy M. Insulin modulates gluconeogenesis by inhibition of the coactivator TORC2. Nature. 2007; 449:366–369. [PubMed: 17805301]

Dunning BE, Gerich JE. The role of alpha-cell dysregulation in fasting and postprandial hyperglycemia in type 2 diabetes and therapeutic implications. Endocrine reviews. 2007; 28:253–283. [PubMed: 17409288]

Eipel C, Abshagen K, Vollmar B. Regulation of hepatic blood flow: the hepatic arterial buffer response revisited. World J Gastroenterol. 2010; 16:6046–6057. [PubMed: 21182219]

Exton JH, Corbin JG, Harper SC. Control of gluconeogenesis in liver. V. Effects of fasting, diabetes, and glucagon on lactate and endogenous metabolism in the perfused rat liver. J Biol Chem. 1972; 247:4996–5003. [PubMed: 5061605]

Formenti F, Constantin-Teodosiu D, Emmanuel Y, Cheeseman J, Dorrington KL, Edwards LM, Humphreys SM, Lappin TR, McMullin MF, McNamara CJ, Mills W, Murphy JA, O'Connor DF, Percy MJ, Ratcliffe PJ, Smith TG, Treacy M, Frayn KN, Greenhaff PL, Karpe F, Clarke K, Robbins PA. Regulation of human metabolism by hypoxia-inducible factor. Proceedings of the National Academy of Sciences of the United States of America. 2010; 107:12722–12727. [PubMed: 20616028]

Gallavan RH Jr, Chou CC. Possible mechanisms for the initiation and maintenance of postprandial intestinal hyperemia. The American journal of physiology. 1985; 249:G301–308. [PubMed: 3898869]

Gelling RW, Du XQ, Dichmann DS, Romer J, Huang H, Cui L, Obici S, Tang B, Holst JJ, Fledelius C, Johansen PB, Rossetti L, Jelicks LA, Serup P, Nishimura E, Charron MJ. Lower blood glucose, hyperglucagonemia, and pancreatic alpha cell hyperplasia in glucagon receptor knockout mice. Proceedings of the National Academy of Sciences of the United States of America. 2003; 100:1438–1443. [PubMed: 12552113]

Gordeuk VR, Miasnikova GY, Sergueeva AI, Niu X, Nouraie M, Okhotin DJ, Polyakova LA, Ammosova T, Nekhai S, Ganz T, Prchal JT. Chuvash polycythemia VHLR200W mutation is associated with down-regulation of hepcidin expression. Blood. 2011; 118:5278–5282. [PubMed: 21876117]

Habegger KM, Heppner KM, Geary N, Bartness TJ, DiMarchi R, Tschop MH. The metabolic actions of glucagon revisited. Nature reviews Endocrinology. 2010; 6:689–697.

Herzig S, Long F, Jhala US, Hedrick S, Quinn R, Bauer A, Rudolph D, Schutz G, Yoon C, Puigserver P, Spiegelman B, Montminy M. CREB regulates hepatic gluconeogenesis through the coactivator PGC-1. Nature. 2001; 413:179–183. [PubMed: 11557984]

Hickey MM, Lam JC, Bezman NA, Rathmell WK, Simon MC. von Hippel-Lindau mutation in mice recapitulates Chuvash polycythemia via hypoxia-inducible factor-2alpha signaling and splenic erythropoiesis. The Journal of clinical investigation. 2007; 117:3879–3889. [PubMed: 17992257]

Jenssen T, Nurjhan N, Consoli A, Gerich JE. Failure of substrate-induced gluconeogenesis to increase overall glucose appearance in normal humans. Demonstration of hepatic autoregulation without a change in plasma glucose concentration. The Journal of clinical investigation. 1990; 86:489–497. [PubMed: 2200805]

Kim C, Cheng CY, Saldanha SA, Taylor SS. PKA-I holoenzyme structure reveals a mechanism for cAMP-dependent activation. Cell. 2007; 130:1032–1043. [PubMed: 17889648]

Koo SH, Flechner L, Qi L, Zhang X, Screaton RA, Jeffries S, Hedrick S, Xu W, Boussouar F, Brindle P, Takemori H, Montminy M. The CREB coactivator TORC2 is a key regulator of fasting glucose metabolism. Nature. 2005; 437:1109–1111. [PubMed: 16148943]

Lee Y, Wang MY, Du XQ, Charron MJ, Unger RH. Glucagon receptor knockout prevents insulin-deficient type 1 diabetes in mice. Diabetes. 2011; 60:391–397. [PubMed: 21270251]

Lewis GF, Vranic M, Giacca A. Glucagon enhances the direct suppressive effect of insulin on hepatic glucose production in humans. The American journal of physiology. 1997; 272:E371–378. [PubMed: 9124541]

Liang Y, Osborne MC, Monia BP, Bhanot S, Gaarde WA, Reed C, She P, Jetton TL, Demarest KT. Reduction in glucagon receptor expression by an antisense oligonucleotide ameliorates diabetic syndrome in db/db mice. Diabetes. 2004; 53:410–417. [PubMed: 14747292]

MacKenzie SJ, Baillie GS, McPhee I, Bolger GB, Houslay MD. ERK2 mitogen-activated protein kinase binding, phosphorylation, and regulation of the PDE4D cAMP-specific phosphodiesterases. The involvement of COOH-terminal docking sites and NH2-terminal UCR regions. J Biol Chem. 2000; 275:16609–16617. [PubMed: 10828059]

McClain DA, Abuelgasim KA, Nouraie M, Salomon-Andonie J, Niu X, Miasnikova G, Polyakova LA, Sergueeva A, Okhotin DJ, Cherqaoui R, Okhotin D, Cox JE, Swierczek S, Song J, Simon MC, Huang J, Simcox JA, Yoon D, Prchal JT, Gordeuk VR. Decreased serum glucose and glycosylated hemoglobin levels in patients with Chuvash polycythemia: a role for HIF in glucose metabolism. Journal of molecular medicine. 2013; 91:59–67. [PubMed: 23015148]

Omori K, Kotera J. Overview of PDEs and their regulation. Circulation research. 2007; 100:309–327. [PubMed: 17307970]

Porksen S, Nielsen LB, Kaas A, Kocova M, Chiarelli F, Orskov C, Holst JJ, Ploug KB, Hougaard P, Hansen L, Mortensen HB. Meal-stimulated glucagon release is associated with postprandial blood glucose level and does not interfere with glycemic control in children and adolescents with new-onset type 1 diabetes. J Clin Endocrinol Metab. 2007; 92:2910–2916. [PubMed: 17519307]

Prabhakar NR, Semenza GL. Oxygen Sensing and Homeostasis. Physiology (Bethesda). 2015; 30:340–348. [PubMed: 26328879]

Qu A, Taylor M, Xue X, Matsubara T, Metzger D, Chambon P, Gonzalez FJ, Shah YM. Hypoxia-inducible transcription factor 2alpha promotes steatohepatitis through augmenting lipid accumulation, inflammation, and fibrosis. Hepatology. 2011; 54:472–483. [PubMed: 21538443]

Ramadoss P, Unger-Smith NE, Lam FS, Hollenberg AN. STAT3 targets the regulatory regions of gluconeogenic genes in vivo. Molecular endocrinology. 2009; 23:827–837. [PubMed: 19264844]

Ramakrishnan SK, Anderson ER, Martin A, Centofanti B, Shah YM. Maternal intestinal HIF-2alpha is necessary for sensing iron demands of lactation in mice. Proceedings of the National Academy of Sciences of the United States of America. 2015; 112:E3738–3747. [PubMed: 26124130]

Ren B, Deng Y, Mukhopadhyay A, Lanahan AA, Zhuang ZW, Moodie KL, Mulligan-Kehoe MJ, Byzova TV, Peterson RT, Simons M. ERK1/2-Akt1 crosstalk regulates arteriogenesis in mice and zebrafish. The Journal of clinical investigation. 2010; 120:1217–1228. [PubMed: 20237411]

Schuler M, Dierich A, Chambon P, Metzger D. Efficient temporally controlled targeted somatic mutagenesis in hepatocytes of the mouse. Genesis. 2004; 39:167–172. [PubMed: 15282742]

Shah YM, Ito S, Morimura K, Chen C, Yim SH, Haase VH, Gonzalez FJ. Hypoxia-inducible factor augments experimental colitis through an MIF-dependent inflammatory signaling cascade. Gastroenterology. 2008; 134:2036–2048. 2048 e2031–2033. [PubMed: 18439915]

Taniguchi CM, Finger EC, Krieg AJ, Wu C, Diep AN, LaGory EL, Wei K, McGinnis LM, Yuan J, Kuo CJ, Giaccia AJ. Cross-talk between hypoxia and insulin signaling through Phd3 regulates hepatic glucose and lipid metabolism and ameliorates diabetes. Nature medicine. 2013; 19:1325–1330.

Tse TF, Clutter WE, Shah SD, Cryer PE. Mechanisms of postprandial glucose counterregulation in man. Physiologic roles of glucagon and epinephrine vis-a-vis insulin in the prevention of hypoglycemia late after glucose ingestion. The Journal of clinical investigation. 1983; 72:278–286. [PubMed: 6135707]

Unger RH, Eisentraut AM, Madison LL. The effects of total starvation upon the levels of circulating glucagon and insulin in man. The Journal of clinical investigation. 1963; 42:1031–1039. [PubMed: 13995385]

Walker JN, Ramracheya R, Zhang Q, Johnson PR, Braun M, Rorsman P. Regulation of glucagon secretion by glucose: paracrine, intrinsic or both? Diabetes, obesity & metabolism. 2011; 13(Suppl 1):95–105.

Wang X, Schneider A. HIF-2alpha-mediated activation of the epidermal growth factor receptor potentiates head and neck cancer cell migration in response to hypoxia. Carcinogenesis. 2010; 31:1202–1210. [PubMed: 20395290]

Wei K, Piecewicz SM, McGinnis LM, Taniguchi CM, Wiegand SJ, Anderson K, Chan CW, Mulligan KX, Kuo D, Yuan J, Vallon M, Morton LC, Lefai E, Simon MC, Maher JJ, Mithieux G, Rajas F, Annes JP, McGuinness OP, Thurston G, Giaccia AJ, Kuo CJ. A liver Hif-2alpha-Irs2 pathway sensitizes hepatic insulin signaling and is modulated by Vegf inhibition. Nature medicine. 2013; 19:1331–1337.

Yap TA, Yan L, Patnaik A, Fearen I, Olmos D, Papadopoulos K, Baird RD, Delgado L, Taylor A, Lupinacci L, Riisnaes R, Pope LL, Heaton SP, Thomas G, Garrett MD, Sullivan DM, de Bono JS, Tolcher AW. First-in-man clinical trial of the oral pan-AKT inhibitor MK-2206 in patients with advanced solid tumors. Journal of clinical oncology : official journal of the American Society of Clinical Oncology. 2011; 29:4688–4695. [PubMed: 22025163]

Zheng L, Kelly CJ, Colgan SP. Physiologic hypoxia and oxygen homeostasis in the healthy intestine. A Review in the Theme: Cellular Responses to Hypoxia. Am J Physiol Cell Physiol. 2015; 309:C350–360. [PubMed: 26179603]
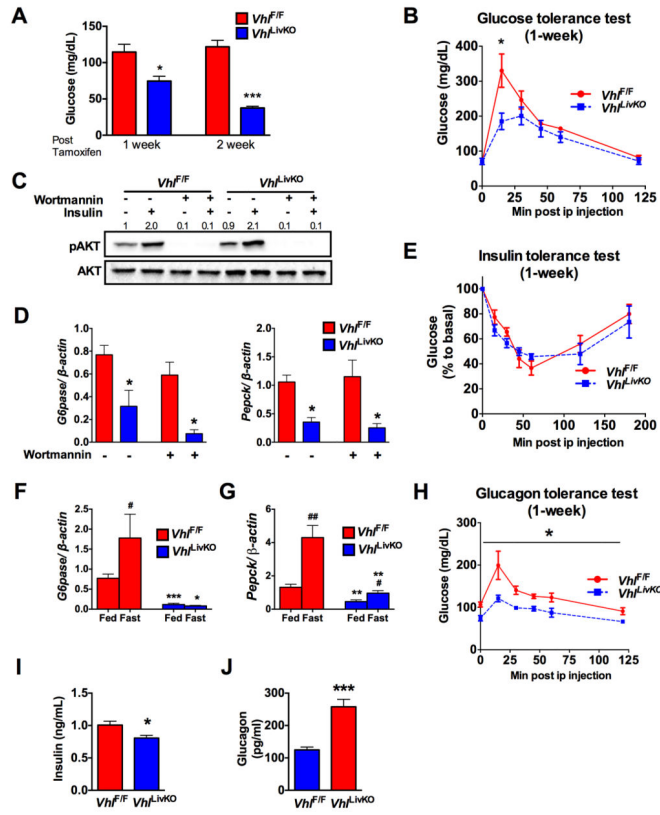
Figure 1. Disruption of hepatic Vhl (Vhl^LivKO) is associated with an attenuated glucagon response

(A) Fasting glucose and (B) glucose tolerance test at 1-week following VHL disruption in the liver (*Vhl*^LivKO). (C) Insulin stimulated AKT phosphorylation and (D) qPCR analysis of *G6pase* and *Pepck* mRNA in PH treated with 100 nM Wortmannin for 2-hours. (E) Insulin tolerance test at 1-week following tamoxifen treatment. (F and G) qPCR analysis in the livers of fed or overnight fasted mice. (H) Glucagon tolerance test at 1-week after VHL disruption. (I) Serum insulin and (J) serum glucagon assessed at 1-week following VHL disruption. Each bar represents the mean± S.E.M. *p < 0.05, **p < 0.01, ***p < 0.001 compared to *Vhl*^F/F. #p < 0.05, ##p < 0.01 compared to Fed. Four to five mice were used per group and experiments with PH were done in triplicates and repeated at least three times.
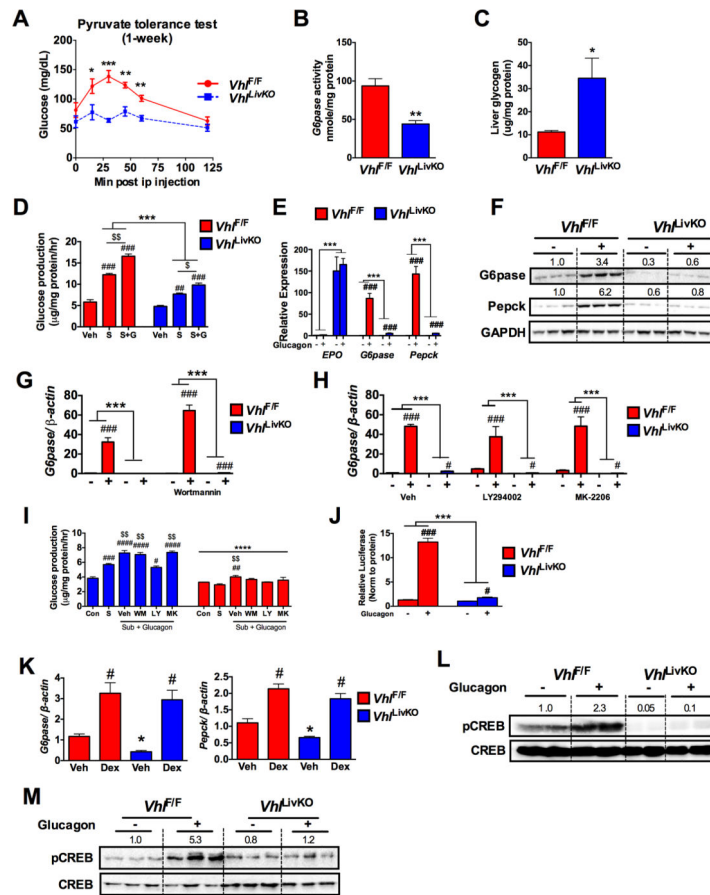
Figure 2. Disruption of hepatic VHL (Vhl^LivKO) decreases hepatic glucagon action and glucose output from liver

(A) Pyruvate tolerance test at 1-week after disruption of VHL in liver (*Vhl*^LivKO). (B) *G6pase* activity and (C) hepatic glycogen content assessed in *Vhl*^F/F and *Vhl*^LivKO mice. *p < 0.05, **p < 0.01, ***p < 0.001 compared to *Vhl*^F/F. (D) *De novo* gluconeogenesis in Vehilcle (Veh), substrate (S) and substrate+glucagon (S+G) treated cells. (E) qPCR analysis for HIF2α target gene, *Epo* mRNA and glucagon induction of *G6pase* and *Pepck* in PH. (F) Western blot analysis of G6Pase and PEPCK in PH treated with 100 nM glucagon for 6-hours. Glucagon-induced *G6pase* expression in PH pre-treated with (G) 50 nM Wortmannin for 2-hours or (H) 50 nM LY294002 or 50 nM MK-2206 for 1-hour. (I) Glucose production in PH pretreated for 1-hour with or without 50 nM Wortmannin or 50 nM LY294002 or 50 nM MK-2206. ***p < 0.001 compared *Vhl*^F/F. # p < 0.05, ###p < 0.001 compared to Vehicle. $p<0.05, $$p < 0.001, $$$p < 0.0001 compared to substrate alone. (J) *G6pase* promoter luciferase assay in PH. Luciferase values were normalized to protein content. (K) qPCR analysis of *G6pase* and *Pepck* in the PH treated with 10 nM dexamethasone for 2-hours. pCREB assessed (L) in vivo and (M) in PH. Each bar represents the mean value ± S.E.M. *p < 0.05, **p < 0.01, ***p < 0.001 compared to *Vhl*^F/F. #p < 0.05, ## p < 0.01, ###p < 0.001 compared to Vehicle. Four to five mice were used per group and the experiments with PH were done in triplicate and repeated at least three times.
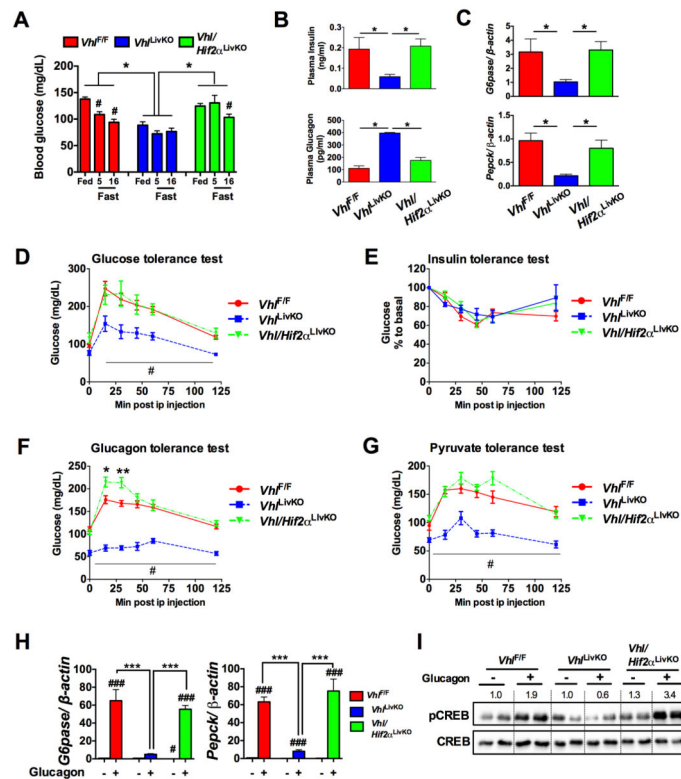
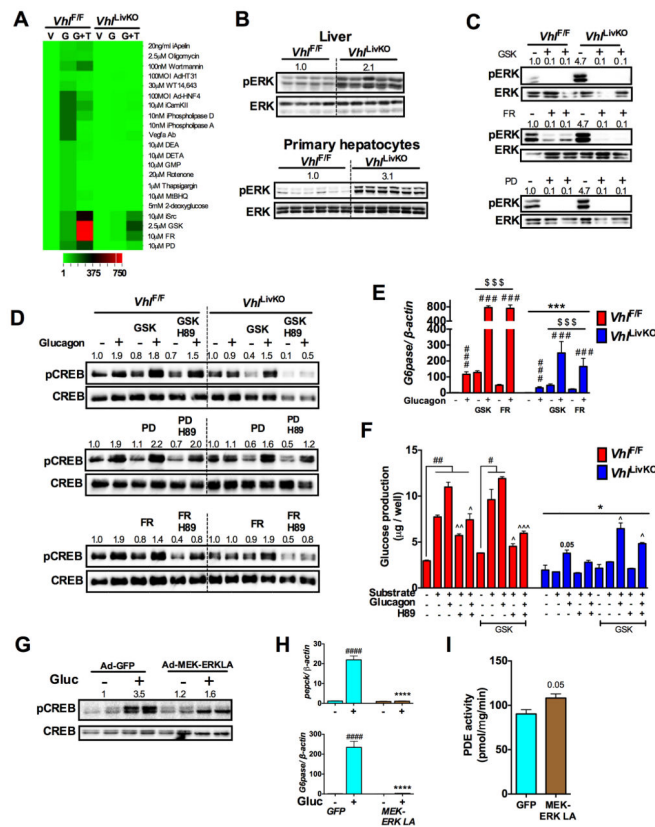**Figure 3. Abrogated glucagon response in Vhl^LivKO mice is HIF2α dependent**

(A) Blood glucose, (B) serum insulin levels (top panel) and serum glucagon levels (bottom panel) assessed at 1-week following tamoxifen treatment. (C) qPCR for *G6pase* and *Pepck* mRNA in the livers of overnight fasted mice. *$p < 0.05$ compared to *Vhl*^LivKO. #$p < 0.05$ compared to Fed. (D) Glucose tolerance, (E) Insulin tolerance, (F) glucagon tolerance and (G) pyruvate tolerance test in *Vhl*^LivKO and *Vhl/Hif2*^LivKO mice. Five to eight mice were assessed per group. *$p < 0.05$, **$p < 0.01$ compared to *Vhl*^F/F. #$p < 0.001$ compared *Vhl*^LivKO. (H) *G6pase* and *Pepck* mRNA expression and (I) pCREB in glucagon treated PH. *** $p < 0.001$ compared to *Vhl*^LivKO; #, $p < 0.05$ compared to Vehicle; ###, $p < 0.001$ compared to Vehicle. Each bar represents the mean value ± S.E.M. Experiments with PH were done in triplicate and repeated at least three times.
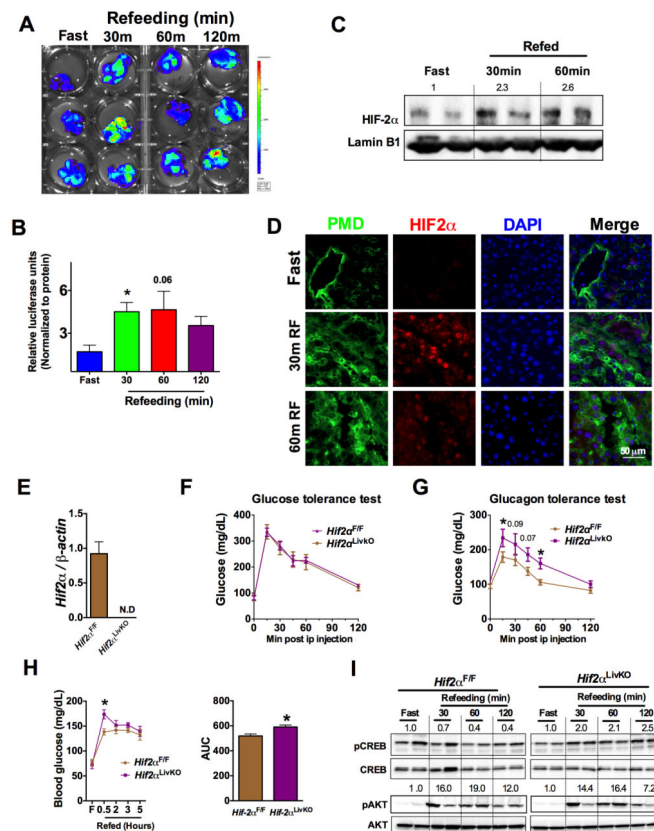
Figure 4. Transient increase in hepatic HIF2α regulates postprandial glucagon action

(A) In vivo imaging of livers and (B) liver tissue luciferase assays in mice fasted overnight or refed for 30-, 60- and 120-minutes. *p < 0.05 compared to fasted. Three mice were assessed per group. (C) Western blot for HIF2α and (D) co-immunostaining for pimonidazole adducts and HIF2α in the overnight fasted and 30 or 60 minutes refed livers. Five mice were assessed per group. (E) qPCR analysis of *Hif2α* mRNA in hepatocytes. (F) Glucose and (G) glucagon tolerance performed in 6-week-old WT and *Hif2α*LivKO mice. (H) Glucose levels monitored in overnight fasted and refed mice. *p < 0.05 compared to *Hif2α*F/F. (I) Western blot analysis for pCREB and pAKT in WT and *Hif2α*LivKO mice fasted overnight and refed for 30-minutes to 2-hours. Six mice were assessed per group.
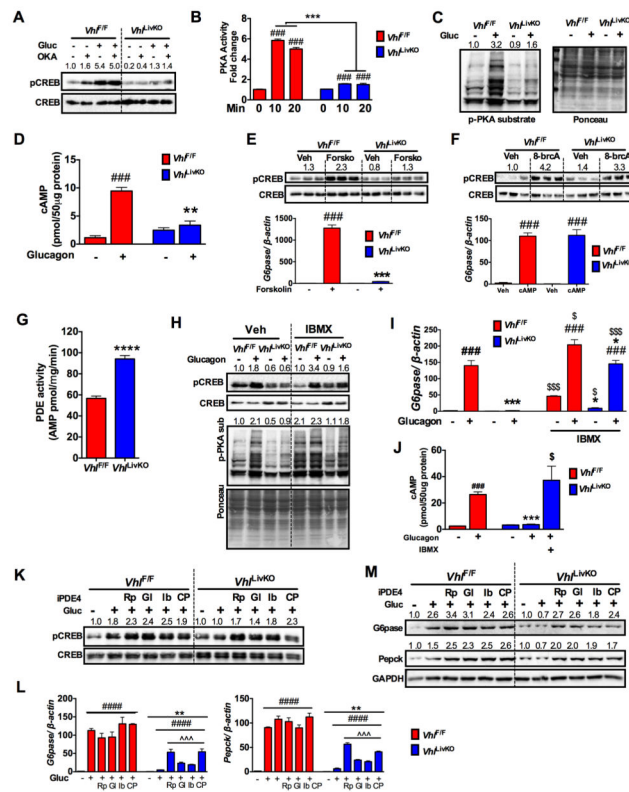
Figure 5. HIF2α represses glucagon-mediated PKA activity by increasing cAMP hydrolysis

(A) Glucagon stimulated pCREB in PH pre-treated with phosphatase inhibitor okadaic acid (200 nM OKA) for 2-hours. (B) PKA activity and (C) Western blot analysis for phospho-PKA (p-PKA) substrates and (D) cAMP levels assessed in PH treated with glucagon. Western blot analysis for pCREB and qPCR for *G6pase* mRNA (bottom panel) in PH treated with (E) 20 μM forskolin or (F) 200 μM 8-br-cAMP for 2-hours. (G) PDE activity assessed by 5′-AMP levels in PH isolated at 1-week following VHL disruption. (H) Glucagon-stimulated pCREB, (I) *G6pase* expression and (J) cAMP levels in PH pretreated with 1 μM IBMX for 1-hour. (K) Glucagon-stimulated pCREB, *G6pase* and *Pepck* (L) mRNA or (M) protein expression (glucagon treatment for 6-hours) in PH pretreated for 16-hours with Rolipram (Rp, 1 μM), Glaucine (Gl, 1 μM), Ibudilast (Ib, 1 μM), and CP80,633 (Cp, 1 μM). PH were treated again with respective PDE inhibitors 30 minutes before glucagon treatment. Experiment with PH were done in triplicates and repeated at least twice. Each bar represents the mean value ± S.E.M. *$p < 0.05$, **$p < 0.05$, ***$p < 0.001$ compared to *Vhl*[F/F]. # $p < 0.05$, ###$p < 0.001$, ####$p < 0.0001$ compared to Vehicle, $$p < 0.05$, $$$$p < 0.001$ are IBMX treated compared to their untreated controls. ^^^$p < 0.001$ compared to no inhibitor treatment.

Figure 6. HIF2α induced ERK activity represses hepatic glucagon signaling

(A) qPCR analysis of *G6pase* in PH pre-treated with inhibitors or activators for two-hours and then with glucagon for additional 2-hours (V-Veh; G- Glucagon; G+T- Glucagon + treatments). (B and C) pERK levels assessed in livers and PH of *Vhl*^LivKO mice. pERK levels, (D) Glucagon induced pCREB and (E) qPCR analysis of *G6pase* mRNA in PH pre-treated with 2.5 μM GSK1120212 and 10 μM PD98059 and10 μMFR180204 for 16-hours. Each bar represents the mean value ± S.E.M. ***p < 0.001 compared to *Vhl*^F/F. ###p < 0.001 compared to no glucagon. $p < 0.05, $$$p < 0.001 compared to without inhibitor treatment. (F) Glucose production in PH pre-treated with GSK for 16-hours. Each bar represents the mean value ± S.E.M. ##p < 0.001 compared to no substrate or glucagon. ^p < 0.05, ^^p <0.01 compared to substrate and glucagon treated, *p <0.05 compared to *Vhl*^F/F $p < 0.05, $$$p < 0.001 compared to without inhibitor treatment. Glucagon stimulated (G) pCREB and (H) *Pepck* and *G6pase* mRNA expression in WT PH infected with Ad-GFP or Ad-MEK-ERK-LA virus for 48-hours. ***p < 0.001 compared to Ad-GFP. ####p < 0.001 compared to no glucagon. (I) PDE activity in PH infected with Ad-GFP or Ad-MEK-ERK-LA virus for 48-hours. Five to six mice were used per group and experiments with PH were done in triplicates and repeated at least twice.
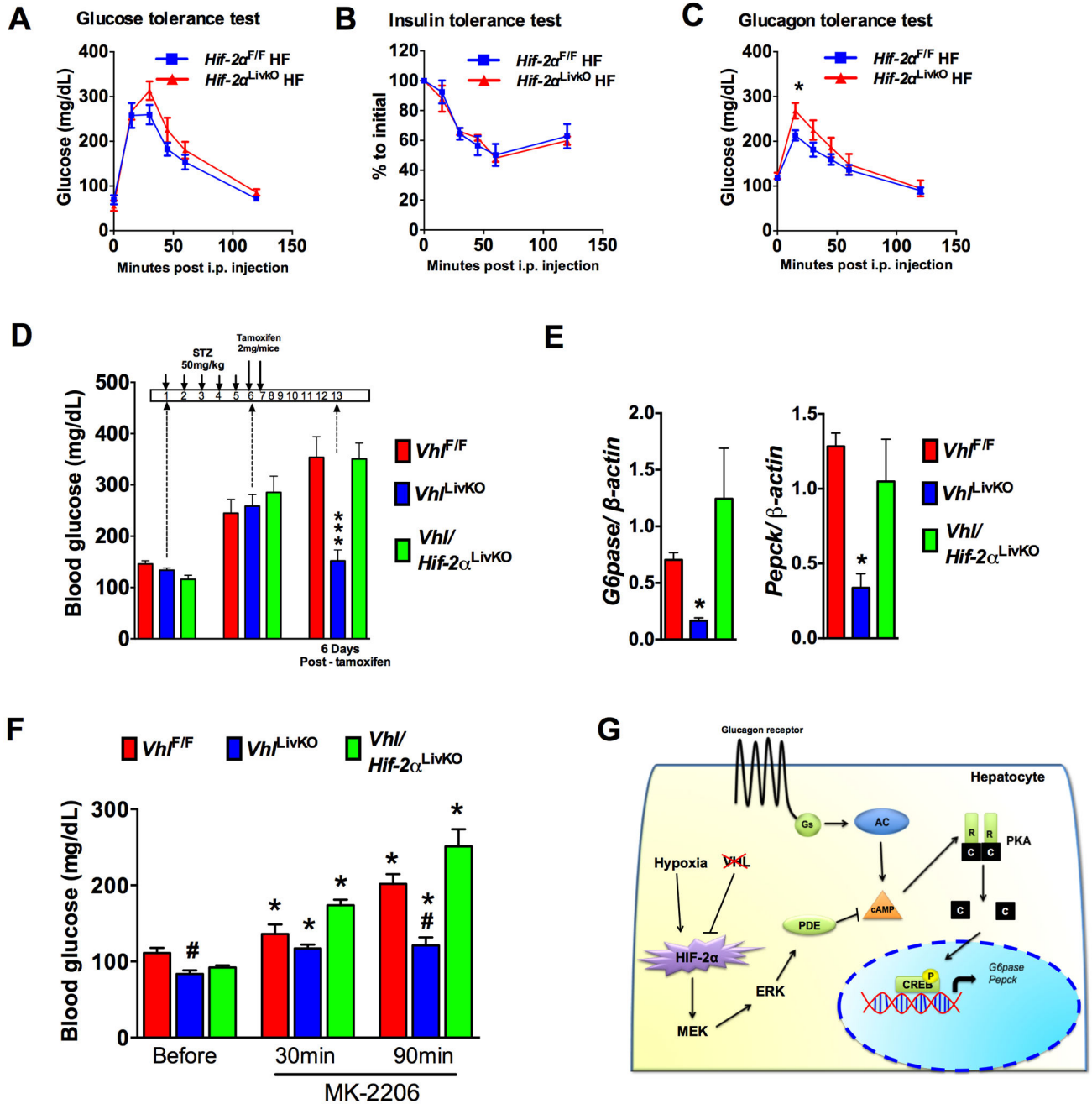
Figure 7. HIF2α mediated repression of glucagon signaling ameliorates hyperglycemia in STZ induced diabetic and insulin resistant mice

(A) Glucose, (B) insulin, (C) glucagon tolerance test performed in $HIF2\alpha^{\text{F/F}}$ and $HIF2\alpha^{\text{LivKO}}$ mice fed a 60% HFD for 6-weeks. *p < 0.05 compared to $HIF2\alpha^{\text{F/F}}$. (D) Blood glucose monitored in STZ treated mice. (E) qPCR analysis for *G6pase* and *Pepck* mRNA in livers of STZ treated mice. *p < 0.05 compared to $Vhl^{\text{F/F}}$, ***p < 0.001 compared to $Vhl^{\text{F/F}}$. Five to seven mice assessed per group. (F) Blood glucose monitored in Vhl^{LivKO} mice injected i.p. with MK-2206 (50mg/kg body weight). *p < 0.05 compared to mice before treatment, #p < 0.05 compared to $Vhl^{\text{F/F}}$. Each bar represents the mean value ± S.E.M. Six

mice to eleven mice were assessed per group. (G) Schematic in which HIF2α-mediated increase in ERK signaling represses glucagon-PKA-CREB signaling through increased PDE-dependent hydrolysis of cAMP in liver.